Proceedings of the 37th Chinese Control Conference
July 25-27, 2018, Wuhan, China

The Design and Implementation of an Underwater Multimode Acoustic Modem for Autonomous Underwater Vehicles

Qi Dong, Yiyin Wang, Xinping Guan
Department of Automation, Shanghai Jiao Tong University, Shanghai 200240, P. R. China
E-mail: ddqq123@sjtu.edu.cn

Abstract: Autonomous underwater vehicles (AUVs) are efficient tools to explore oceans. Communication is a fundamental function of AUVs, therefore the development of underwater acoustic modems has drawn a great deal of attention. In this paper, the design and implementation of an underwater multimode acoustic modem for AUVs is presented. The modem contains two types of demodulations, noncoherent and coherent demodulation. Furthermore, a power selection strategy is integrated in the modem to fulfill the requirements of AUVs. We have experimentally evaluated the modem prototype in the lab and field.

Key Words: Underwater Acoustic Modems, Underwater Acoustic Communication

1 Introduction

AUVs are efficient tools to explore oceans [1], particularly in unapproachable and unpredictable areas, AUVs are expected to complete various tasks, such as underwater mapping, search and rescue operations, and so on. The acoustic communication capability is in demand for autonomous underwater vehicles (AUVs) to send data, receive commands and cooperate with others. Compared with wired communications, the wireless acoustic communications enable AUVs working more flexibly and covertly. Thus, acoustic modems implemented communication algorithms and network protocols is one of the core equipment for AUVs.

In recent years, various hardware implementations of underwater acoustic modems are available [2]. Demirors et al have proposed a software defined acoustic modem (S-RAM) which is based on universal software radio peripheral (USRP) [3, 4]. In [5], H.Yan et al realized a digital signal processor (DSP) based orthogonal frequency division multiplexing (OFDM) modem for high-data rate underwater acoustic communications. The MicroModem developed by the woods hole oceanographic institution (WHOI) has phase-shift keying (PSK) and frequency-hopped frequency-shift keying (FH-FSK) modulations [6, 7]. An reconfigurable underwater acoustic modem (r-modem) has been developed with a flexible physical layer in [8].

The goal of this paper is the development of an underwater acoustic modem to be equipped with AUVs. Energy-limited AUVs require the modem to be small and energy-efficient. Since AUVs execute tasks in various environments, various modulation schemes are required to be integrated in the modem. The modem is implemented on OMAPL138, which is a low-power processor based on an ARM and a DSP core. The power selection strategy is implemented on the ARM part, while the digital signal processing is implemented on the DSP part. Since the underwater acoustic communication is challenging and complex, both noncoherent and coherent scheme are integrated on the modem to deal with doubly selective underwater acoustic channels [9, 10]. For the noncoherent scheme, multiple frequency-shift keying (MFSK) is selected for its proved robustness in low-data rate underwater acoustic communications [11]. For the coherent scheme, OFDM techniques [12] combined with quadrature phase-shift keying (QPSK) and quadrature amplitude modulation (QAM) has been adopted in the modem to build a high-data rate communication link by efficient bandwidth utilization. In order to address the power-hungry problem in AUVs, an adaptive power control strategy is proposed. Making use of the feedback from the receiver, the transmitter selects the minimum power that can achieve reliable communication. Finally, we describe experiments conducted in Qiandao lake and an anechoic tank and show several experiments results of the modem prototype.

Part of this work was supported by the National Nature Science Foundation of China under the grants 61773264, 61633017, and 61471237, and the United Fund of Department of Equipment Development and Ministry of Education of China under 6141A02033317.

2 Modem Development

This section is divided into four parts: hardware platform, communication modules, signal structure, power selection strategy. The communication modules and signal structure are implemented in the DSP part of the hardware, while the power selection strategy is executed on the ARM part.

2.1 Hardware Platform

The hardware platform block diagram of the prototype is depicted in Fig. 1. The modem is implemented on a small and low-cost platform named OMAPL138, which is suitable for carrying and integrating into other underwater equipment. The OMAPL138 which consists of an ARM926EJ-S core and a C674x DSP core is the heart of the modem [15]. The high-speed digital signal processing including modulation and demodulation, encoding and decoding, synchronization and so on are implemented on the DSP part of the OMAPL138. The ARM part is in charge of interaction with external devices such as control units of AUVs by TCP/IP protocol as the modem has provided an ethernet port. The two processors communication with each other by the shared random access memory (RAM). The modem board is shown in Fig. 2(a). Fig. 2(b) shows the transducer which transforms electric signals into acoustic wave. The transducer which could either receives or transmits signals operates in the 11-14 kHz frequency band.

2.2 Communication Modules

The modules of the transmitter and receiver implemented in the prototype are depicted in Fig. 3(a) and Fig. 3(b),

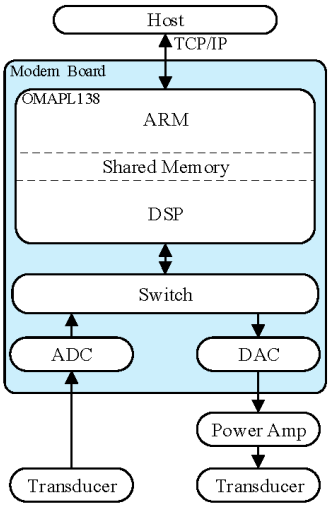

Fig. 1: The hardware platform block diagram of the modem

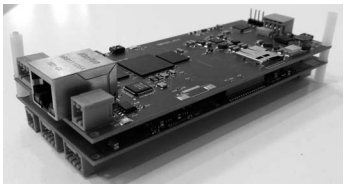

(a) The modem board

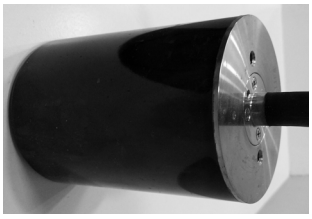

(b) The transducer

Fig. 2: Prototype of the acoustic modem

respectively.

In the transmitter, the source data are encoded by the concatenation code of rate-1/2 convolutional code and rate-1/3 hadamard code to help error detection and correction for reducing BER. Moreover, cyclic redundancy check (CRC) and interleaved coding are utilized to ensure correctness of the data. The encoded data is modulated and the preamble is added as discussed in Section 2.3. Upsampling and pulse shaping are essential to make the transmitted signal fit in the effective bandwidth. A square-root-raised-cosine filter is applied for pulse shaping block to minimize intersymbol interference. The up conversion block is to convert the baseband to the passband signal for digital to analog converter (DAC) block.

In the receiver, opposite processes are carried out to deal with the signal, excluding detection and synchronization. In the detection and synchronization block, the energy of signals is calculated to test whether the signals arrive. The preamble is used to synchronize the frames by cross-correlation. The location of maximum correlation value shows where the preamble is. Moreover, the viterbi algorithm [13] is utilized for the decoding of convolutional code.

2.3 Signal Structure

Fig. 4 shows the structure of a data frame, which is divided into three parts: the preamble, the space time and the data payload. The preamble which is used for detection and synchronization is a short sequence. In the modem, the linear frequency modulated (LFM) signal, more commonly referred to as the chirp signal, is selected for the preamble due to its good autocorrelation properties. The guard time is added between the preamble and the data payload in order to ensure that the preamble does not affect the data payload due to multipath channels. Both the noncoherent and coherent scheme can be selected for the data payload. For noncoherent scheme, MFSK, which is a traditional modulation mode with the lowest data rate and the greatest robustness is utilized. For coherent scheme, OFDM modulation combined with QPSK, QAM16 and QAM64 can be selected. In OFDM modulation, the symbol duration is long compared to the multipath spread of the channel, because the available bandwidth has been divided into a large number of orthogonal subbands. Thus, OFDM has advantages to combat frequency selective fading and enable high rate transmissions.

Each of OFDM symbols consists of two parts: the cyclic prefix (CP) and the data payload. The CP helps to eliminate the ISI and facilitates the easy equalization. Moreover, received signals are equalized by pilot subcarriers through the least-squares (LS) algorithm. One of the four modulation schemes can be selected to modulate the source data according to the channel condition. The basic parameters for the CP-OFDM are listed in Table. 1. The corresponding data rates for the four transmission modes are listed in Table. 2.

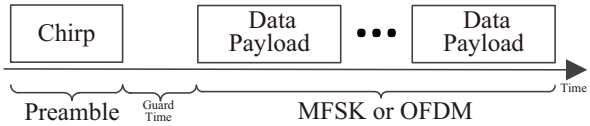

Fig. 4: A frame

Table 1: CP-OFDM Parameters

DAC sampling rate	$f_s = 200\ kHz$
Center frequency	$f_c = 12.5\ kHz$
Bandwidth	$B = 3\ kHz$
Subcarrier spacing	$\Delta f = 25\ Hz$
Symbol time	$T_s = 40\ ms$
Duration of the CP	$T_{cp} = 8.125\ ms$
Number of subcarriers	$K = 256$

Table 2: Transmission Rate of Each Modulation Mode

Modulation mode	MFSK	QPSK	QAM16	QAM64
Transmission rate(bits/s)	208	1230	2480	3730

2.4 Power Selection Strategy

Because AUVs have limited power and cannot be easily recharged underwater, the power-hungry problem is severe. Thus, how to find an appropriate communication power to balance communication performance and energy consumption should also be considered. We implement a simple media access control (MAC) protocol that can support

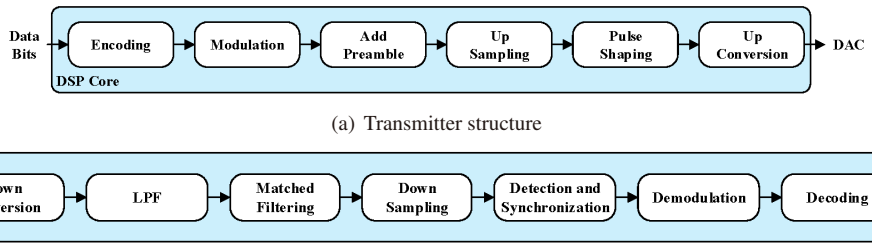

(a) Transmitter structure

(b) Receiver structure

Fig. 3: Structure of the underwater acoustic modem

the power selection strategy for the acoustic communications between two modems. The MAC protocol allows the TX node to receive a binary chirp spread-spectrum (B-CSS) signal from the RX node for feedback [3, 14, 16]. The B-CSS signal is reliability and robust in severe multipath and Doppler effected underwater acoustic channel. The up-chirp feedback signal requires the TX node to increase the power. On the other hand the down-chirp feedback signal requires the TX node to reduce the power. The feedback continues, until an appropriate communication power is found.

Fig. 5 depicts the power selection strategy between 2 stations via B-CSS signal.

1) Start with an initial modulation mode mod, initial transmission power P_{init} and step P_{step}.
2) Set the valid range of signal to noise ratio (SNR) for every modulation. Define $i(mod, low)$ and $i(mod, high)$ as the lowest and highest SNR for mod, respectively.
3) The transmitter sends data via P_{init}.
4) The receiver estimates the SNR of received signals as $rSNR$. If $rSNR < i(mod, low)$, the receiver feedbacks an up-chirp signal to the transmitter. If $rSNR > i(mod, high)$, the receiver feedbacks a down-chirp signal. If $i(mod, low) \leq rSNR \leq i(mod, high)$, the receiver doesn't feedback chirp signals.
5) The transmitter detects chirp signals via cross-correlation. If the up-chirp signal is detected, the power will be increased as $P_{init} = P_{init} + P_{step}$. If the down-chirp signal is detected, the power will be decreased as $P_{init} = P_{init} - P_{step}$.
6) Turn to the third step.

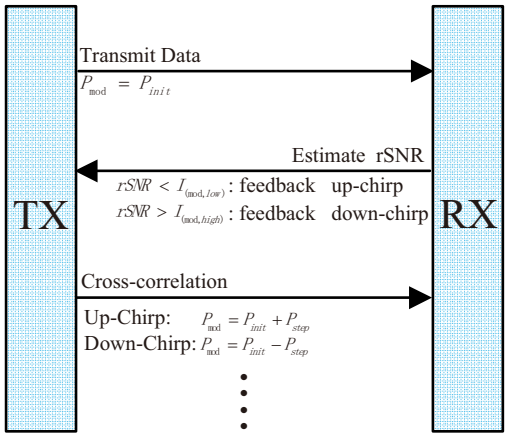

Fig. 5: The power selection strategy

3 Experimental Results

In this section, we test communicating functionalities of the modem in Qiandao lake. Besides, we also discuss the modem's BER performance experimented in an anechoic tank.

3.1 Qiandao Lake Experiments

Fig. 6 shows that we test communication function of the modem in Qiandao lake. The distance between the transmitter and receiver is 100 meters, the depth is 2 meters. Text messages, such as "hello underwater world" are transmitted and received successfully by MFSK modulate. The coherent demodulation can work only if the distance is less than 10 meters.

Fig. 6: Functional tests in Qiandao lake

3.2 BER Performance

The performance of the modem is evaluated by the experiments conducted in an anechoic tank with the size of $20 \times 8 \times 8$ m^3. The distance between two transducers is 10 m at the depth of 3 m. We change the SNR through power adjustment and calculate the BER during the experiments. The SNR is given by

$$SNR = 10 \log(P_s / P_n) \quad (1)$$

where P_s is the power of the signal and P_n is the power of the noise.

Fig. 7 depicts the received signal in time and frequency domain after QPSK modulation while SNR is 4.9 dB. The transmitted preamble and the guard interval could be clearly identified. In this experiment, we estimate the SNR of the received signal through the difference of the signal segment and the noise segment in the signal strength. Specifically, let us denote $s[n]$ as the received signal during the signal transmission, and $w[n]$ as the received signal during the silent

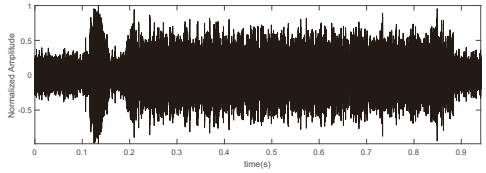

(a) Received signals in time domain

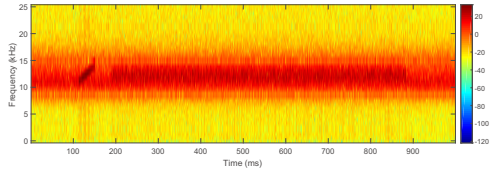

(b) Received signals in frequency domain

Fig. 7: Received QPSK signal

period. $\frac{P_s}{P_n}$ is calculated as

$$\frac{P_s}{P_n} = \frac{E\{|s[n]|^2\} - E\{|w[n]|^2\}}{E\{|w[n]|^2\}} \tag{2}$$

The experimental results are presented in Fig. 8. Fig. 8(a) shows the BER while the modulation mode is MFSK and QPSK. It is clear that compared to QPSK, a low BRE could still be obtained through MFSK when the SNR is low. The BER of QAM16 and QAM64 is tested with the aid of amplifier and shown in Fig. 8(b). We could increase the SNR of signal through the power adjustment conducted by the amplifier. According to the experimental results, the signal can be decoded when SNR is above a certain threshold no matter which modulation mode is adopted.

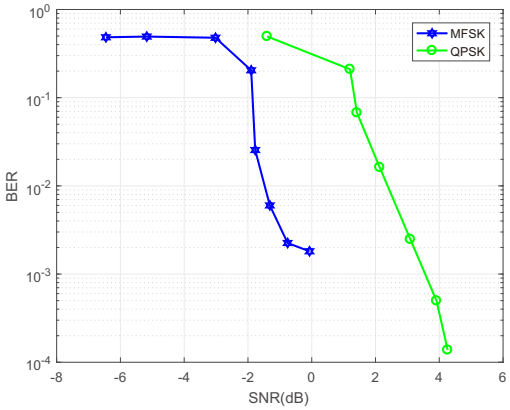

(a) BER of MFSK and QPSK (without power amplifier)

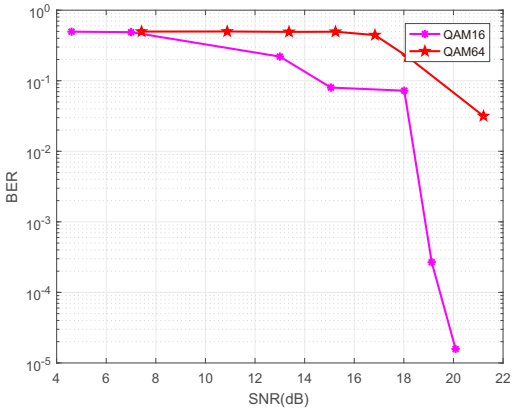

(b) BER of QAM16 and QAM64 (with power amplifier)

Fig. 8: Experimental results

4 Conclusion

We present the design, implementation, and experimental results of an underwater multimode acoustic modem which is small-sized and low-powered for AUVs. Furthermore, the modem integrates a power selection strategy. The details of the physical communication algorithm and the hardware implementation platform are described in this paper. Finally, experiments are conducted to evaluate the proposed modem in the field (the Qiandao lake) and the lab (an anechoic water tank).

5 Acknowledgement

I wish to express my heartfelt gratitude to Professor Xiaoli Ma for her help on experimental design.

References

[1] J. Yuh, G. Marani, and D. R. Blidberg, Applications of marine robotic vehicles, Intell. Service Robot., 4(4): 221-231, 2011.

[2] H. S. Dol, P. Casari, T. van der Zwan, and R. Otnes, Software-defined underwater acoustic modems: Historical review and the NILUS approach, IEEE J. Ocean. Eng., 42(3): 722-737, 2017.

[3] E. Demirors, G. Sklivanitis, G. E. Santagati, T. Melodia, and S. N. Batalama, Design of a software-defined underwater acoustic modem with real-time physical layer adaptation capabilities, in Proc. ACM Int. Conf. UnderWater Netw. Syst. (WUWNet), 2014: 25.

[4] E. Demirors, G. Sklivanitis, T. Melodia, S. N. Batalama, and D. A. Pados, Software-defined underwater acoustic networks: toward a high-rate real-time reconfigurable modem, IEEE Commun. Mag., 53(11): 64-71, 2015.

[5] H. Yan, L. Wan, S. Zhou, Z. Shi, J.-H. Cui, J. Huang, and H. Zhou, DSP based receiver implementation for OFDM acoustic modems, Elsevier J. Phys. Commun, 5(1): 22-32, 2012.

[6] L. Freitag, M. Grund, S. Singh, J. Partan, P. Koski, and K. Ball, The WHOI micro-modem: an acoustic communications and navigation system for multiple platforms, in Proc. IEEE OCEANS, 2005: 1086-1092.

[7] E. Gallimore, J. Partan, I. Vaughn, S. Singh, J. Shusta, and L. Freitag, The WHOI micromodem-2: A scalable system for acoustic communications and networking, in Proc. IEEE OCEANS, 2010: 1-7.

[8] M. Aydinlik, A. T. Ozdemir, and M. Stajanovic, A physical layer implementation on reconfigurable underwater acoustic modem, in Proc. IEEE OCEANS, 2008: 1-4.

[9] M. Chitre, S. Shahabudeen, and M. Stojanovic, Underwater acoustic communications and networking: Recent advances and future challenges, Marine Tech. Soc. J., 42(1): 103-116, 2008.

[10] M. Stojanovic and J. Preisig, Underwater acoustic communication channels: Propagation models and statistical characterization, IEEE Commun. Mag., 47(1): 84-89, 2009.

[11] K. F. Scussel, J. A. Rice, and S. Merriam, A new MFSK acoustic modem for operation in adverse underwater channels, in Proc. IEEE OCEANS, 1997: 247-254.

[12] B. Li, S. Zhou, M. Stojanovic, L. Freitag, and P. Willett, Multicarrier communication over underwater acoustic channel-

s with nonuniform doppler shifts, IEEE J. Ocean. Eng., 33(2): 198-209, 2008.
[13] A. Viterbi, Error bounds for convolutional codes and an asymptotically optimum decoding algorithm, IEEE Trans. Inf. Theory, 13(2): 260-269, 1967.
[14] H. Lee, T. H. Kim, J. W. Choi, and S. Choi, Chirp signalbased aerial acoustic communication for smart devices, in Proc. IEEE INFOCOM, 2015: 2407-2415.
[15] T. Instrument, OMAP-L138 technical reference manual, www.ti.com, 2009.
[16] J. A. Neasham, G. Goodfellow, and R. Sharphouse, Development of the "seatrac" miniature acoustic modem and USBL positioning units for subsea robotics and diver applications, in Proc. IEEE OCEANS, 2015: 1-8.